DOI 10.31489/2021Ph3/83-92
UDC 68.004.05

N.I. Kosach[1], V.B. Bolshakov[2], I.T. Bohdanov[3], Y.O. Suchikova[3*]

[1]State Enterprise KHARKIV MACHINERY PLAN «FED», Kharkiv, Ukraine;
[2]Civil organization «Ukraienian Academy of Metrology», Kyiv, Ukraine;
[3]Berdyansk State Pedagogical University, Ukraine
([*]yanasuchikova@gmail.com)

Statistical evaluation of morphological parameters of porous nanostructures on the synthesized indium phosphide surface

A constructive method for estimating the surface morphology of nanostructured semiconductors, which consists in determining the main statistical characteristics of the aggregate structure of nanoscale objects on their synthesized surface is presented. In terms of the indium phosphide semiconductor with a synthesized porous layer on its surface, it is shown that the evaluation of the main statistical characteristics allows a deeper understanding of the kinetics of the pore formation process during typical electrochemical treatment of the crystal. The determination of the main statistical metrologically based characteristics (indicators of the distribution center, variation, and shape of the distribution) allows us to understand in more detail view the processes occurring during electrochemical processing of crystals. In the long run, this will make it possible to create nanostructures with predetermined properties, which will become the basis for the industrial production of high-quality nanostructured semiconductors.

Keywords: synthesis, semiconductors, surface morphology, measurement, aggregate structure, statistical analysis, indium phosphide, ImageJ.

Introduction

Currently, nanotechnology is the industry demonstrating the fastest development rates. It is widely used to create ultra-fast and super-powerful computers [1, 2], in electronics (lasers, photonics) [3], alternative energy [4, 5], information technologies (information transmission and storage) [6], environmental monitoring (wastewater, air, soil) [7], as well as in a number of other utmost relevant applied aspects of science and technology [8, 9].

The necessity for this is that nanomaterials are characterized, as a rule, by a much larger proportion of surface atoms, which determine the dominant features of the physical and chemical properties of materials [10]. Thus, structuring the surface of semiconductors leads to an increase of their effective area by tenfolds, which has an important practical consequence for improving the efficiency of photo-emmissive energy converters [11, 12]. In addition, quantum-dimensional effects begin to appear at the submicron level [13]. This property is possessed by quantum dots [14, 15], nanoconductors [16], nanowires [17], porous layers [18], etc.

In this regard, the synthesis of nanostructures with specified functional characteristics and, first of all, controlled sizes of nanoobjects remains as a crucial problem in recent decades. This is emphasized in such program documents as «Strategic Research and Innovation Agenda for Nanomedicine, European Technology Platform on Nanomedicine, 2016–2030» [19], «EU US Roadmap Nanoinformatics, 2017–2030» [20], «Continuing to Protect the Nanotechnology Workforce: NIOSH Nanotechnology Research Plan for 2018–2025» [21].

The complexity of solving this problem is due to the fact that two competing mechanisms always operate during the formation of surface nanostructures: the nanostructures generation with specified properties

[22] and the self-organization of nanoobjects [23]. Overcoming this contradiction is possible only with a complete, detailed analysis of the statistical characteristics of the synthesized surface morphology, the most promising tool for which is the analysis of microscopic images of the surface of nanomaterials using statistical methods [24].

The article presents the results of representative metrologically based studies of the surface morphology of a nanostructured semiconductor, namely, the establishment of statistical characteristics of the pore distribution over diameter in a typical process of nanostructure synthesis, which, along with previously obtained results of the trend of their dependence on etching time [25], allows creating crystals with a predetermined aggregate structure.

Methods and materials

The surface morphology of a nanostructured semiconductor during its synthesis was studied experimentally on the example of a sample of n-type single-crystal indium phosphide (por-InP) with surface orientation (111) [26]. Porous surface layers of indium phosphide were obtained by typical electrochemical etching of a sample in a hydrochloric acid solution ($10H_2O$+1HCl). The etching time t = 20 min, current density of j = 150 mA/cm^2. Plates of indium monocrystalline phosphide were polished before etching and cleaned with alcohol and vinegar. The pores on the plate were formed in a standard electrolytic cell with platinum at the cathode [27]. After this they were dried in air and subjected to short-term drawing in a nitrogen stream to stabilize the properties. The morphology of the synthesized nanoobjects was studied using a JEOL-6490 raster electron microscope with a resolution of up to 3.0 nm, accelerating voltage (0.3–30) kW; magnification from x5 to x300,000; types of contrast (secondary and reflected electrons): topographic, compositional, and shadow.

For representativeness of the experiment, 10 crystal plates were examined and 5 observations of the morphology of nanoobjects on the surface of each sample were made, the results of which were within the limits of confidence intervals of ± 5 % for the measured value P = 0.95.

Raster processing of photomicrographs under surface analysis based on selected morphological characteristics was performed using the ImageJ program. Statistical processing of results was performed using the Origin Pro program.

The main tasks of analyzing photomicrographs of the surface of nanostructured samples are:

- statistical processing of the obtained in the measurement process of objects parameters;
- determination of the average values of the values obtained;
- the construction of graphic dependences for visualization of the analysis process.

A two-dimensional image, obtained using a microscope, in a certain approximation could be considered as a matrix, the indexes of which describe the numbers of rows and columns, and the numerical values of elements characterize the color intensity. The main parameter that characterizes a digital image is its resolution (the number of pixels in the original image and the color depth).

The morphological parameter used for the analysis is the average pore diameter, despite the fact that the pores have a cone shape-the diameter of their Don is less than the diameter of the surface section, for simplicity of research, but without losing the generality and correctness of the results obtained, it was considered that they have a cylindrical shape in the lumbar section.

For statistical estimation of the pore distribution by diameter the values of the indicators of the average diameter series in ascending order were ranked and sorted. To estimate the distribution series the main statistical indicators of the distribution center are found: the mode, median, and simple arithmetic mean of its value, as well as indicators of variation in the pore distribution series over the diameter. The change in the variation of the distribution of the series over the diameter in the aggregate was carried out using absolute and relative indicators, which were determined by calculating the asymmetry coefficients, Pearson, and the access indicator.

Results and Discussion

Figure 1 shows a typical micrography obtained using a microscope of the studied fragment of one of the samples. Visual analysis of photomicrograph shows that the synthesized surface of indium phosphide is densely covered with pores. The pores shape the tracks. The nature of these tracks are micro-scratches on the surface of the plate [28]. They can also be caused by uneven impurity distribution and the crystallographic orientation of the semiconductor plate [29]. Along the track line, the pores tend to merge and form long channels [30]. Isolated pores are mostly cylindrical in cross-section. Some areas have massive etched pits, the appearance of which is most often associated with the release of dislocation to the surface [31, 32].

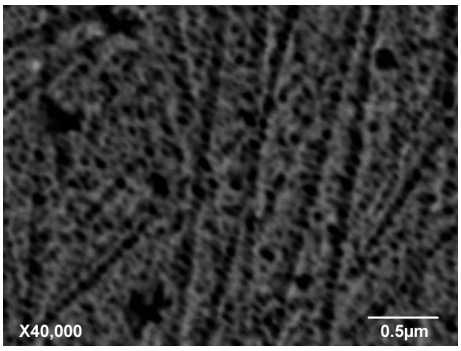

Figure 1. Morphology of *por-InP:*

Figure 2 shows the raster processing of microphotograph performed in the ImageJ program. To increase the contrast of the pore borders, a Bandpass filter based on Fourier transform is used allowing to remove both high and low spatial frequencies in the image [33]. The Watershed algorithm is used to separate adjacent crystallites and pores with indistinct boundaries [34].

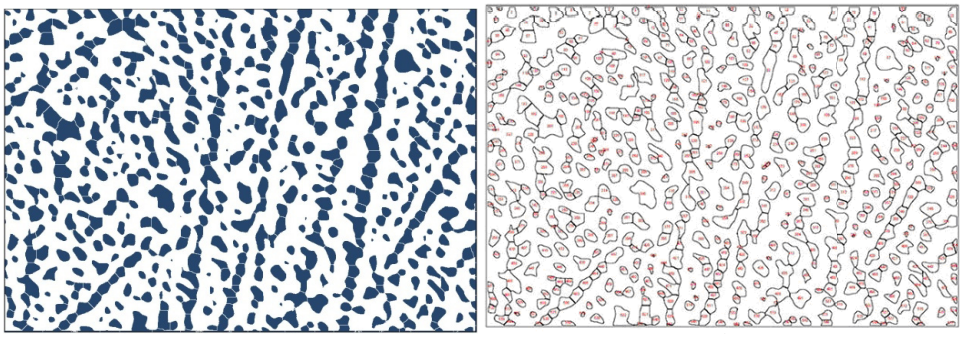

a) b)

Figure 2. Results of processing a microscopic image of the sample surface using the ImageJ program
a) after the binarization process, b) after using the Watershed algorithm

For the studied sample fragment the number of pores was calculated (there were 558 of them) and their size distribution $R_N = [d_{min}, d_{max}]$ (Fig. 3), where $N = 6$ is the number of distributions, $d_{\min}$ and $d_{\max}$ are the minimum and maximum pore diameter in microns. For statistical estimation of the pore distribution by diameter it is necessary to rank and sort the value of the indicators of the average diameter series in ascending order.

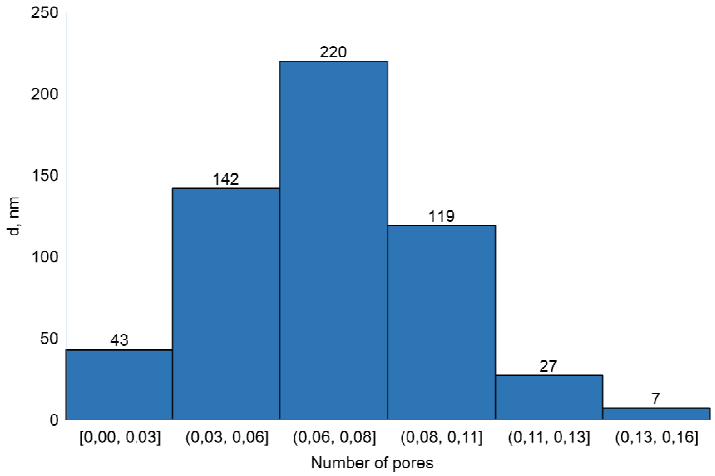

Figure 3. Histogram of pore distribution by size

To estimate the range of pore diameter distribution by size the above-mentioned indicators were defined as follows.

Indicators of the distribution center. This class of indicators includes: the simple arithmetic mean of pores — ($\overline{d}$); the most common value of the average diameter — the mode (M_o) and the diameter value that falls in the middle of an ordered population — the median (M_e), which serves as a good characteristic in an asymmetric distribution of data, because even in the presence of outliers of data it is more resistant to their influence. In symmetric distribution series the values of the mode and median coincide with the average pore value [35]:

$$\overline{d} = M_e = M_o, \tag{1}$$

and in moderately asymmetric ones, they correlate as follows [36]:

$$3(\overline{d} - M_e) \approx \overline{d} - M_o\,. \tag{2}$$

The indicators of the distribution center obtained from the results of the performed studies are presented in Table 1.

Table 1

Indicators of the distribution center of a number of pore diameters

Indicator	Identification	Value, μm
Arithmetic mean of the diameter, $\overline{d}$	$\overline{d} = \frac{\sum_{i=1}^{n} d_i}{n}$	0.0683
Mode, M_o	The most common diameter value is the number of repetitions f = 86	0.07136
Median, M_e	the value of the diameter that divides the sizes of the pore distribution series by diameter into two parts	0.07136

Thus, you can state that the mode and median of the series coincide, but exceed the average value. Such a series is considered conditionally symmetric.

Variation indicators. This class of indicators is presented in Table 2. Its study is of great practical importance and is a necessary component in the variational analysis. This is due to the fact that the average, being equal in effect, performs its main task with different degrees of accuracy: the smaller the differences in individual values of the attribute to be averaged, the more homogeneous is its total value, and, consequently, the more accurate and reliable the average value is, and vice versa [37]. Therefore, by the degree of variation, we can judge the variation limits in the pore diameter, the homogeneity of the total value of diameter values.

Table 2

The variation indicators of the pore distribution series by the diameter

Indicator	Identification	Formula	Value
1	2	3	4
Invariable indicators of variation			
Variation span, μm	Difference between maximum and minimum pore diameter values	$R = d_{\max} - d_{\min}$	0.1564074
Mean deviation, μm^2	Arithmetic mean from absolute divergences of individual pore diameter values from the overall average	$\overline{D} = \frac{\sum \lvert d - \overline{d} \rvert f}{\sum f}$	0.0222
Dispersion, μm^2	The arithmetic mean of the deviation squares of each pore diameter value from the arithmetic mean value	$\sigma^2 = \frac{\sum \left(d - \overline{d}\right)^2 f}{\sum f}$	0.000821
Mean square deviation, μm	STD	$\sigma = \sqrt{\sigma^2}$	0.0286
Fixed dispersion, μm^2	Capable estimate of the variance	$s^2 = \frac{\sum \left(d_i - \overline{d}\right)^2}{n-1}$	0.00552
Estimation of the mean square deviation, μm	The square root of the fixed variance	$s = \sqrt{s^2}$	0.0743

1	2	3	4
Relative indicators of variation			
Coefficient of variation, %	Measure of the relative spread of total values: shows what percentage of the average pore diameter is its average spread	$\nu = \frac{\sigma}{d}$	41.92
Relative linear deflection, %	Characterizes the proportion of the average value of pore diameters of absolute divergences from the average quantity	$K_d = \frac{D}{\overline{d}}$	32.48

In Table: f — the sum of the frequencies of variation in the series, and n — the number of features.

Thus, the results of these studies allow us to conclude that since the coefficient of variation is greater than 30 %, but less than 70 %, there is a moderate variation in the pore diameters of the synthesized semiconductor surface.

Indicators of the distribution form. One of the main characteristics of the distribution form is its symmetry, that is, when the frequencies of any two variants equidistant on both sides of the distribution center are equal to each other; in any other case, the distribution is considered unbalanced. The criterion for the degree of symmetry of the distribution is the asymmetry coefficient [38]:

$$A_s = \frac{M_3}{s^3}, \tag{3}$$

where *M3* is the central moment of the third order of the pore diameter distribution series, s — mean-square deviation.

The central moments of the pore distribution series by diameter calculated from the results of the measurements performed are shown in Figure 4.

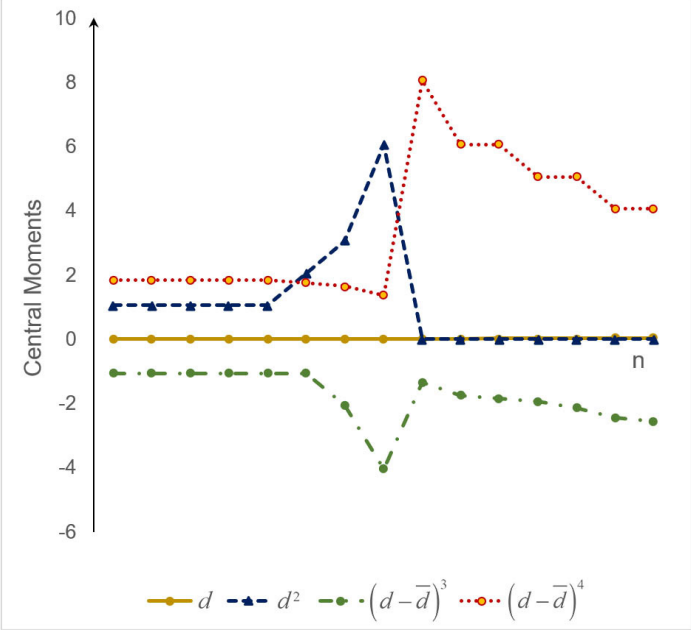

Figure 4. Diagram of the central moments distribution to determine the significance of the skewness of the pore diameter distribution series

It is determined that in our case A_s = 4.254, which indicates that there is a right-sided asymmetry in the resulting distribution.

The significance of the skewness indicator was determined using the mean square error of the skewness ratio [39, 40]:

$$s_{As} = \sqrt{\frac{6(n-2)}{(n+1)(n+3)}}. \tag{4}$$

In this case it is considered that if $|A_s|/s_{As} \prec 3$ then the asymmetry is insignificant, its presence is explained by random circumstances. If $|A_s|/s_{As} \succ 3$, then the asymmetry is considered significant and the distribution of the feature in the general population is not symmetric.

As a result of the analysis of the measurements performed it was found that s_{As} = 0.171, i.e., $|A_s|/s_{As} = 4.254 : 0.171 = 24.93 \succ 3$, and it can be argued that in the study there is a significant asymmetry of distribution: larger pores predominate in this fragment of the porous surface, and pores with dimensions smaller than the average diameter are much rarer. This correlates with the previously obtained result [25]: the number of pores and their size distribution depends on the time of crystal etching — the longer the processing of the crystal, the greater the number of primordial pores will appear on the surface. In general, the effect of the synthesis time (t, min) on the size (d, μm) of the pore mass of the corresponding trend equation has the following form [25]:

$$d = 0.143\ t^2 + 4.447\ t — 10.779. \quad (5)$$

Obtained structural skewness indicators allow us to assess the skewness only in the central part of the distribution, that is, in the main mass of sizes, where they do not depend on the boundary values. However, despite this, such characteristics are an important element in the analysis of the pore distribution by size, as they help to analyze the main mass of the pores, and do not take into account those pores that are unprovable, such as germ pores, which are still very small in size, and massive pores, which are classified as etching pits, resulting from the digestion of surface defects and dislocations in a typical method of electrochemical synthesis.

Conclusions

Experimental studies of the surface morphology of nanostructured semiconductors are carried out on the example of a synthesized porous layer on an indium phosphide crystal. Representative metrologically capable results were obtained using the most efficient modern software tools for analyzing microscopic images and statistical methods.

As a result, the characteristics of one of the main parameters of the aggregate structure of the synthesized porous layer are determined — the pore diameter distribution on semiconductors during their electrical etching, namely the median (M_e = 0.07136 μm), mode (M_o = 0.07136 μm) and the arithmetic mean diameter ($\bar{d}$ = 0.0683 μm), on the basis of which it is concluded that the pore diameter distribution series is conditionally symmetric.

This variation was found to be moderate. Structural indicators of skewness allowed us to establish an important element of the pore growth mechanism which correlates with previously obtained results [25] — the longer the crystal is processed, the greater the number of primordial pores will appear on the surface, the greater the pore size spread.

Thus, the presented methodology can become an effective tool for the characterization of porous nanostructures on the crystal surface, and the results obtained are an important link in the structural analysis of nanostructured semiconductors. In the future they can ensure the formation of nanostructures with adjustable properties and quality levels, which is a solution to a complex technological problem of our time.

Acknowledgments

The work was carried out as part of the state budget research «Theoretical and methodological foundations of the systemic fundamentalization of the training of future specialists in the field of nanomaterials knowledge for productive professional activity» (state registration number 0121U109426).

References

1 Karoui F.S. Application of quantum mechanics for computing the vibrational spectra of nitrogen complexes in silicon nanomaterials / F.S. Karoui, A. Karoui // Some Applications of Quantum Mechanics. — 2012. — P. 131.

2 Ouyang J. Application of nanomaterials in two-terminal resistive-switching memory devices / J. Ouyang // Nano reviews. — 2010. — Vol. 1. — № . 1. — P. 5118.

3 Zhukovskii Y.F. Influence of F centres on structural and electronic properties of AlN single-walled nanotubes / Y.F. Zhukovskii et al. // Journal of Physics: Condensed Matter. — 2007. — 19: 39. — P. 395021.

4 Suchikova Y.O. Sulfide passivation of indium phosphide porous surfaces / Y.O. Suchikova // Journal of Nano-and Electronic Physics. — 2017. –9:1. — P. 1006–1.

5 Chernov S.A. Photo-and thermo-stimulated luminescence of CsI—Tl crystal after UV light irradiation at 80 K / S.A. Chernov, L. Trinkler, A.I. Popov // Radiation effects and defects in solids. — 1998. –143: № 4. — P. 345–355.

6 Park K.D. Radiative control of dark excitons at room temperature by nano-optical antenna-tip Purcell effect / K.D. Park, T. Jiang, G. Clark, X. Xu, M.B. Raschke // Nature nanotechnology. — 2018. — 13: 1. — P. 59–64.

7 Yu G. Applications of Nanomaterials for Heavy Metal Removal from Water and Soil: A Review / G. Yu, X. Wang, J. Liu // Sustainability. — 2021. –13: 2. — P. 713.

8 Zhukovskii Y.F. Structural and electronic properties of single-walled AlN nanotubes of different chiralities and sizes / Y.F. Zhukovskii // Journal of Physics: Condensed Matter. — 2006. — Vol. 18. — № 33. — P. S2045.

9 Eglitis R.I. Semi-empirical simulations of the electron centers in MgO crystal / R.I. Eglitis // Computational materials science. — 1996. — Vol. 5. — № 4. — P. 298–306.

10 Bayati M. R. A photocatalytic approach in micro arc oxidation of WO3–TiO2 nano porous semiconductors under pulse current / M.R. Bayati, F. Golestani-Fard, A. Z. Moshfegh, R. Molaei // Materials Chemistry and Physics. — 2011. — Vol. 128. — № 3. — P. 427–432.

11 Zhan W. Recent progress on engineering highly efficient porous semiconductor photocatalysts derived from Metal–organic frameworks / W. Zhan, L. Sun, X. Han // Nano-micro letters. — 2019. — Vol. 11. — № 1. — P. 1.

12 Serikov T.M. The effect of electric transport properties of titanium dioxide nanostructures on their photocatalytic activity / T.M. Serikov // Bulletin of the university of Karaganda-Physics. — 2020. — 99(3). — 13 — 21.

13 BorodinY. V. Spectroscopy of nanoscale crystalline structural elements / Y.V. Borodin, K.V. Sysolov, V.R. Rande, G.V. Vavilova, O. Starý // Bulletin of the university of Karaganda-Physics. — 2020. — 99(3). — P. 46–53.

14 Alavi M. Functionalized carbon-based nanomaterials and quantum dots with antibacterial activity: a review / M. Alavi, E. Jabari, E. Jabbari // Expert Review of Anti-infective Therapy. — 2021. — Vol. 19. — № . 1. — P. 35–44.

15 Frieler M. Effects of Doxorubicin Delivery by Nitrogen-Doped Graphene Quantum Dots on Cancer Cell Growth: Experimental Study and Mathematical Modeling / M. Frieler, C. Pho, B.H. Lee // Nanomaterials. — 2021. — Vol. 11. — № 1. — P. 140.

16 Pan D. TiB nano-whiskers reinforced titanium matrix composites with novel nano-reticulated microstructure and high performance via composite powder by selective laser melting / D. Pan //Materials Science and Engineering: A. — 2021. — Vol. 799. — P. 140137.

17 Vambol S. O. Formation of filamentary structures of oxide on the surface of monocrystalline gallium arsenide / S.O. Vambol et al. // Journal of Nano-and Electronic Physics. — 2017. — V. 9. — № 6.

18 Suchikova J.A. Synthesis of indium nitride epitaxial layers on a substrate of porous indium phosphide / J.A. Suchikova // Journal of Nano-and Electronic Physics. — 2015. — Vol. 7. — № 3. — P. 3017–1.

19 Allon I. Building the European Nanomedicine Research and Innovation Area: EuroNanoMed. 10 years funding innovative research projects / I. Allon, N. Levine, I. Baanante // Precision Nanomedicine. — 2019. — Vol. 2. — № 2. — P. 270–277.

20 Lobaskin, V., Puzyn, T., & Verheyen, G. EU US roadmap nanoinformatics 2030. EU Nanosafety Cluster. — 2018.

21 Hodson, L., Geraci, C., & Schulte, P. Continuing to protect the nanotechnology workforce: NIOSH nanotechnology research plan for 2018–2025. — 2019.

22 Lazarenko A.S. Nanotopography and grain-boundary migration in the vicinity of triple junctions / A.S. Lazarenko et al. // Acta metallurgica et materialia. — 1995. — Vol. 43. — № 2. — P. 639–643.

23 Suchikova Y.A. Influence of dislocations on the process of pore formation in n-InP (111) single crystals / Y.A. Suchikova, V.V. Kidalov, G.A. Sukach // Semiconductors. — 2011. — Vol. 45. — № 1. — P. 121–124.

24 Boyd R.D. New approach to inter-technique comparisons for nanoparticle size measurements; using atomic force microscopy, nanoparticle tracking analysis and dynamic light scattering / R.D. Boyd, S.K. Pichaimuthu, A. Cuenat // Colloids and Surfaces A: Physicochemical and Engineering Aspects. — 2011. — Vol. 387. — № 1–3. — P. 35–42.

25 Suchikova Y. Synthesized nanostructures formation time effect on their morphological quality indicators–pore diameter increase in nanostructured coatings / Y. Suchikova, N. Kosach, V. Bolshakov, G. Shishkin // Ukrainian Metrological Journal. — 2020. — № . 4. — P. 43–49.

26 Suchikova Y.A. Influence of type anion of electrolit on morphology porous inp obtained by electrochemical etching / Y.A. Suchikova, V.V. Kidalov, G.A. Sukach // Journal of Nano- and Electronic Physics. — 2009. — Vol. 1. — № . 4. — P. 78–86.

27 Sychikova Y.A. Dependence of the threshold voltage in indium-phosphide pore formation on the electrolyte composition / Y.A. Sychikova, V. V. Kidalov, G.A. Sukach //Journal of Surface Investigation. X-ray, Synchrotron and Neutron Techniques. — 2013. — Vol. 7. — № . 4. — P. 626–630.

28 Li G. Ag quantum dots modified hierarchically porous and defective TiO2 nanoparticles for improved photocatalytic CO2 reduction / G.Li et al. //Chemical Engineering Journal. — 2021. — Vol. 410. — P. 128397.

29 Li Y. Bulk Si production from Si–Fe melts by directional-solidification, part II: Element distribution / Y. Li et al. // Materials Science in Semiconductor Processing. — 2021. — Vol. 128. — P. 105754.

30 Notthoff C. Swift heavy ion irradiation of GaSb: From ion tracks to nanoporous networks / C. Notthoff et al. // Physical Review Materials. — 2020. — Vol. 4. — № 4. — P. 046001.

31 Massabuau F. C.P. Dislocations as channels for the fabrication of sub-surface porous GaN by electrochemical etching / F.C.P. Massabuau et al. //APL Materials. — 2020. — Vol. 8. — № 3. — P. 031115.

32 Liang H. Solution growth of screw dislocation driven α-GaOOH nanorod arrays and their conversion to porous ZnGa2O4 nanotubes / H. Liang et al. // Chemistry of Materials. — 2017. — Vol. 29. — № 17. — P. 7278–7287.

33 Rueden C.T. et al. ImageJ2: ImageJ for the next generation of scientific image data / C.T. Rueden et al. //BMC bioinformatics. — 2017. — Vol. 18. — № 1. — P. 1–26.

34 Chen Y. A convenient method for quantifying collagen fibers in atherosclerotic lesions by ImageJ software / Y. Chen, Q. Yu, C.B. Xu // Int J Clin Exp Med. — 2017. — Vol. 10. — № 10. — P. 14904–14910.

35 Hoseinzadeh A. The Skew-Reflected-Gompertz distribution for analyzing symmetric and asymmetric data / A. Hoseinzadeh et al. // Journal of Computational and Applied Mathematics. — 2019. — Vol. 349. — P. 132–141.

36 Tsoukalas I. Simulation of stochastic processes exhibiting any-range dependence and arbitrary marginal distributions / I. Tsoukalas, C. Makropoulos, D. Koutsoyiannis // Water Resources Research. — 2018. — Vol. 54. — № 11. — P. 9484–9513.

37 Newey W.K. Asymmetric least squares estimation and testing / W.K. Newey, J.L. Powell // Econometrica: Journal of the Econometric Society. — 1987. — P. 819–847.

38 Jones M.C. Sinh-arcsinh distributions / M.C. Jones, A. Pewsey // Biometrika. — 2009. — Vol. 96. — № 4. — P. 761–780.

39 Zabolotnii S.V. et al. Polynomial estimates of measurand parameters for data from bimodal mixtures of exponential distributions / S.V. Zabolotnii, V.Y. Kucheruk, Z.L. Warsza, A.K. Khassenov // Bulletin of the university of Karaganda-Physics. — 2018. — Vol. 2. — № 90. — P. 71–80.

Н.И. Косач, В.Б. Большаков, И.Т. Богданов, Я.А. Сычикова

Индий фосфидінің синтезделген бетіндегі кеуекті наноқұрылымдардың морфологиялық параметрлерін статистикалық бағалау

Наноқұрылымды жартылай өткізгіштердің беттік морфологиясын бағалаудың конструктивті әдісі ұсынылған, ол олардың синтезделген бетіндегі наноөлшемді объектілердің жиынтық құрылымының негізгі статистикалық сипаттамаларын анықтаудан тұрады. Бетінде синтезделген кеуекті қабаты бар индий фосфидті жартылай өткізгіштің мысалын пайдаланып, негізгі статистикалық сипаттамаларды бағалау кристалды әдеттегі электрохимиялық өңдеу кезінде кеуектерді қалыптастыру процесінің кинетикасын тереңірек түсінуге мүмкіндік беретіндігі көрсетілген. Негізгі статистикалық метрологиялық негізделген сипаттамаларды анықтау (таралу орталығының көрсеткіштері, вариациясы және таралу формасы) кристалдарды электрохимиялық өңдеу кезінде болатын процестерді толығырақ түсінуге мүмкіндік береді. Болашақта бұл алдын ала анықталған қасиеттері бар наноқұрылымдарды құруға мүмкіндік береді және жоғары сапалы наноқұрылымды жартылай өткізгіштердің өнеркәсіптік өндірісіне негіз болады.

Кілт сөздер: синтез, жартылай өткізгіштер, беттік морфология, өлшемдер, агрегаттық құрылым, статистикалық талдау, индий фосфиді, ImageJ.

Н.И. Косач, В.Б. Большаков, И.Т. Богданов, Я.А. Сычикова

Статистическая оценка морфологических показателей пористых наноструктур на синтезированной поверхности фосфида индия

Представлен конструктивный метод оценки морфологии поверхности наноструктурированных полупроводников, который заключается в определении основных статистических характеристик агрегатной структуры наноразмерных объектов на их синтезированной поверхности. На примере полупроводника фосфида индия с синтезированным пористым слоем на его поверхности показано, что оценка основных статистических характеристик позволяет глубже понять кинетику процесса порообразования при типичной электрохимической обработке кристалла. Определение основных статистических метрологически обоснованных характеристик (показателей центра распределения, вариации и формы распределения) позволяет более детально понять процессы, происходящие во время электрохимической обработки кристаллов. В перспективе это позволит создавать наноструктуры с заранее определенными свойствами, станет основой для промышленного изготовления наноструктурированных полупроводников высокого уровня качества.

Ключевые слова: синтез, полупроводники, морфология поверхности, измерения, агрегатная структура, статистический анализ, фосфид индия, ImageJ.

References

1 Karoui, F.S., & Karoui, A. (2012). Application of quantum mechanics for computing the vibrational spectra of nitrogen complexes in silicon nanomaterials. *Some Applications of Quantum Mechanics*, 131.

2 Ouyang, J. (2010). Application of nanomaterials in two-terminal resistive-switching memory devices. *Nano reviews*, *1(1),* 5118.

3 Zhukovskii, Y.F., Pugno, N., Popov, A.I., Balasubramanian, C., & Bellucci, S. (2007). Influence of F centres on structural and electronic properties of AlN single-walled nanotubes. *Journal of Physics: Condensed Matter*, *19(39),* 395021.

4 Suchikova, Y.O. (2017). Sulfide Passivation of Indium Phosphide Porous Surfaces, *Journal of Nano- and Electronic Physics*, *9(1)*, 1006–1–1006–6.

5 Chernov, S.A., Trinkler, L., & Popov, A.I. (1998). Photo-and thermo-stimulated luminescence of CsI—Tl crystal after UV light irradiation at 80 K. *Radiation effects and defects in solids, 143(4)*, 345–355.

6 Park, K.D., Jiang, T., Clark, G., Xu, X., & Raschke, M.B. (2018). Radiative control of dark excitons at room temperature by nano-optical antenna-tip Purcell effect. *Nature nanotechnology, 13(1)*, 59–64.

7 Yu, G., Wang, X., Liu, J., Jiang, P., You, S., Ding, N., ... & Lin, F. (2021). Applications of Nanomaterials for Heavy Metal Removal from Water and Soil: *A Review. Sustainability, 13(2)*, 713.

8 Zhukovskii, Y.F., Popov, A.I., Balasubramanian, C., & Bellucci, S. (2006). Structural and electronic properties of single-walled AlN nanotubes of different chiralities and sizes. *Journal of Physics: Condensed Matter, 18(33),* S2045.

9 Eglitis, R.I., Kuklja, M.M., Kotomin, E.A., Stashans, A., & Popov, A.I. (1996). Semi-empirical simulations of the electron centers in MgO crystal. *Computational materials science, 5(4)*, 298–306.

10 Bayati, M.R., Golestani-Fard, F., Moshfegh, A.Z., & Molaei, R. (2011). A photocatalytic approach in micro arc oxidation of WO3–TiO2 nano porous semiconductors under pulse current. *Materials Chemistry and Physics, 128(3)*, 427–432.

11 Zhan, W., Sun, L., & Han, X. (2019). Recent progress on engineering highly efficient porous semiconductor photocatalysts derived from Metal–organic frameworks. *Nano-micro letters, 11(1),* 1.

12 Serikov, T.M. (2020). The effect of electric transport properties of titanium dioxide nanostructures on their photocatalytic activity. *Bulletin of the university of Karaganda-Physics, 99(3),* 13 — 21. Retrieved from DOI 10.31489/2020Ph3/13–21

13 Borodin, Y.V., Sysolov, K.V., Rande, V.R., Vavilova, G.V., & Starý, O. (2020). Spectroscopy of nanoscale crystalline structural elements. *Bulletin of the university of Karaganda-Physics, 99(3)* 46 — 53. Retrieved from DOI 10.31489/2020Ph3/46–53

14 Alavi, M., Jabari, E., & Jabbari, E. (2021). Functionalized carbon-based nanomaterials and quantum dots with antibacterial activity: a review. *Expert Review of Anti-infective Therapy, 19(1)*, 35–44.

15 Frieler, M., Pho, C., Lee, B.H., Dobrovolny, H., Akkaraju, G.R., & Naumov, A.V. (2021). Effects of Doxorubicin Delivery by Nitrogen-Doped Graphene Quantum Dots on Cancer Cell Growth: Experimental Study and Mathematical Modeling. *Nanomaterials, 11*, 140.

16 Pan, D., Zhang, X., Hou, X., Han, Y., Chu, M., Chen, B., ... & Li, S. (2021). TiB nano-whiskers reinforced titanium matrix composites with novel nano-reticulated microstructure and high performance via composite powder by selective laser melting. *Materials Science and Engineering: A, 799,* 140137.

17 Vambol, S.O., Bohdanov, I.T., Vambol, V.V. & Onyschenko, S.V. (2017). Formation of filamentary structures of oxide on the surface of monocrystalline gallium arsenide. *Journal of Nano-and Electronic Physics, 9(6)*. 06016

18 Suchikova, J.A. (2015). Synthesis of indium nitride epitaxial layers on a substrate of porous indium phosphide. *Journal of Nano-and Electronic Physics, 7(3)*, 3017–1.

19 Allon, I., Levine, N., & Baanante, I. (2019). Building the European Nanomedicine Research and Innovation Area: EuroNanoMed. *10 years funding innovative research projects.* Retrived from DOI:10.33218/PRNANO2(1).190404.1

20 Lobaskin, V., Puzyn, T., & Verheyen, G. (2018). EU US roadmap nanoinformatics 2030. *EU Nanosafety Cluster.*

21 Hodson, L., Geraci, C., & Schulte, P. (2019). Continuing to protect the nanotechnology workforce: NIOSH nanotechnology research plan for 2018–2025.

22 Lazarenko, A.S., Mikhailovskij, I.M., Rabukhin, V.B., & Velikodnaya, O.A. (1995). Nanotopography and grain-boundary migration in the vicinity of triple junctions. *Acta metallurgica et materialia, 43(2), 639–643.*

23 Suchikova, Y.A., Kidalov, V.V., & Sukach, G.A. (2011). Influence of dislocations on the process of pore formation in n-InP (111) single crystals. *Semiconductors, 45(1),* 121–124.

24 Boyd, R.D., Pichaimuthu, S.K., & Cuenat, A. (2011). New approach to inter-technique comparisons for nanoparticle size measurements; using atomic force microscopy, nanoparticle tracking analysis and dynamic light scattering. *Colloids and Surfaces A: Physicochemical and Engineering Aspects, 387(1–3)*, 35–42.

25 Suchikova, Y., Kosach, N., Bolshakov, V., & Shishkin, G. (2020). Synthesized nanostructures formation time effect on their morphological quality indicators–pore diameter increase in nanostructured coatings. *Ukrainian Metrological Journal, 4,* 43–49.

26 Suchikova, Y.A., Kidalov, V.V., & Sukach, G.A. (2009). Influence of type anion of electrolit on morphology porous inp obtained by electrochemical etching. *Journal of Nano- and Electronic Physics, 1(4),* 78–86.

27 Sychikova, Y.A., Kidalov, V.V., & Sukach, G.A. (2013). Dependence of the threshold voltage in indium-phosphide pore formation on the electrolyte composition. *Journal of Surface Investigation. X-ray, Synchrotron and Neutron Techniques, 7(4),* 626–630.

28 Li, G., Sun, Y., Zhang, Q., Gao, Z., Sun, W., & Zhou, X. (2021). Ag quantum dots modified hierarchically porous and defective TiO2 nanoparticles for improved photocatalytic CO_2 reduction. *Chemical Engineering Journal, 410,* 128397.

29 Li, Y., Lei, X., Liu, C., & Zhang, L. (2021). Bulk Si production from Si–Fe melts by directional-solidification, part II: Element distribution. *Materials Science in Semiconductor Processing, 128,* 105754.

30 Notthoff, C., Jordan, S., Hadley, A., Mota-Santiago, P., Elliman, R.G., Lei, W., et al. (2020). Swift heavy ion irradiation of GaSb: From ion tracks to nanoporous networks. *Physical Review Materials, 4(4),* 046001.

31 Massabuau, F.C.P., Griffin, P.H., Springbett, H.P., Liu, Y., Kumar, R.V., Zhu, T., et al. (2020). Dislocations as channels for the fabrication of sub-surface porous GaN by electrochemical etching. *APL Materials, 8(3),* 031115.

32 Liang, H., Meng, F., Lamb, B. K., Ding, Q., Li, L., Wang, Z., et al. (2017). Solution growth of screw dislocation driven α-GaOOH nanorod arrays and their conversion to porous $ZnGa_2O_4$ nanotubes. *Chemistry of Materials, 29(17),* 7278–7287.

33 Rueden, C.T., Schindelin, J., Hiner, M.C., DeZonia, B.E., Walter, A.E., Arena, E.T., et al. (2017). ImageJ2: ImageJ for the next generation of scientific image data. *BMC bioinformatics, 18(1),* 1–26.

34 Chen, Y., Yu, Q., & Xu, C.B. (2017). A convenient method for quantifying collagen fibers in atherosclerotic lesions by ImageJ software. *Int J Clin Exp Med, 10(10),* 14904–14910.

35 Hoseinzadeh, A., Maleki, M., Khodadadi, Z., & Contreras-Reyes, J. E. (2019). The Skew-Reflected-Gompertz distribution for analyzing symmetric and asymmetric data. *Journal of Computational and Applied Mathematics, 349,* 132–141.

36 Tsoukalas, I., Makropoulos, C., & Koutsoyiannis, D. (2018). Simulation of stochastic processes exhibiting any-range dependence and arbitrary marginal distributions. *Water Resources Research, 54(11),* 9484–9513.

37 Carstensen, J., & Lindegarth, M. (2016). Confidence in ecological indicators: a framework for quantifying uncertainty components from monitoring data. *Ecological indicators, 67,* 306–317.

38 Newey, W.K., & Powell, J.L. (1987). Asymmetric least squares estimation and testing. Econometrica: *Journal of the Econometric Society*, 819–847.

39 Jones, M.C., & Pewsey, A. (2009). Sinh-arcsinh distributions. *Biometrika, 96(4),* 761–780.

40 Zabolotnii, S.V., Kucheruk, V.Y., Warsza, Z.L., & Khassenov, A.K. (2018). Polynomial estimates of measurand parameters for data from bimodal mixtures of exponential distributions. *Bulletin of the university of Karaganda-Physics, 2(90),* 71–80.